Chapter 15
Flutter Analysis of Control Surface Free-play by Using a 3-DOF Airfoil Model

İzzet Uluğ and Ender Cigeroglu

Abstract The phenomenon of flutter in aeroelastic systems remains a critical area of research due to its implications for the safety of aircraft wings. Free-play, modeled by using a piecewise linear approach to examine its effect on the aeroelastic response of a system, is a common nonlinearity in control surfaces, which occurs due to gaps at the joints in the control mechanisms. This paper investigates the flutter characteristics of a 3-DOF airfoil model with free-play between plunge and flap motions. The equation of motion (EOM) is obtained via Lagrange's equations, and Theodorsen approach is employed for aerodynamic loads. The EOM can be solved by various methods, namely the harmonic balance method (HBM) and the describing function method (DFM), which can be used in the frequency domain, as well as time integration methods. In this study, DFM is used due to frequency domain methods being more efficient compared to time domain methods. Flutter instability is determined by varying the airspeed and identifying the equivalent damping of the system where the airspeed that causes the damping value of zero is the flutter speed searched. A parametric study is conducted to evaluate the effects of varying free-play gap sizes on the flutter characteristics. The results indicate that free-play changes the flutter speed and mode, with a reduction in the flutter boundary compared to the linear case. Additionally, the study examines nonlinear flutter boundaries, focusing on the development of limit cycle oscillations (LCOs) due to free-play.

Keywords Flutter · Free-play · Nonlinear Flutter · Limit Cycle Oscillations (LCOs) · Aeroelastic Instability

Introduction

Flutter is a type of aeroelastic instability that arises from the interaction of structural, aerodynamic, and inertial forces, leading to an increase in vibrations. This oscillatory instability occurs when aerodynamic forces couple with the natural vibration modes of the structure, potentially resulting in dangerous, self-sustaining oscillations. Nonlinearities, both structural and aerodynamic, play a critical role in influencing the flutter behavior of a system. One common structural nonlinearity is free-play, which emerges due to gaps or looseness in the hinge mechanisms of control surfaces. Free-play significantly alters the flutter characteristics, potentially introducing limit cycle oscillations (LCOs), as shown in studies by Dowell and Tang [1]. Yu et al. [2] conducted a numerical study analyzing the impact of free-play nonlinearity on flutter and LCOs by using 2-DOF airfoil models, showing how free-play influences flutter behavior and the occurrence of LCOs. This type of structural nonlinearity has been a key focus in many aeroelastic studies, since it changes how the stiffness in control surfaces behaves depending on the displacement. This leads to complex flutter behavior that cannot be captured by linear models alone. For instance, Conner et al. [3] demonstrated how free-play introduces nonlinear dynamics that lead to periodic oscillations and other behaviors beyond the flutter boundary. Similarly, Irani et al. [4] further confirmed that an increase in the gap results in consistent decrease in flutter speed, emphasizing the importance of considering these effects early in the design phases. These structural nonlinearities affect both the flutter speed and the post-flutter behavior of the system, making it critical to account for them in flutter analysis.

Traditionally, time-domain methods have been used to analyze flutter by simulating the response of the system over time. While these methods provide detailed insights into transient and steady-state behaviors, they can be computationally

İzzet Uluğ · Ender Cigeroglu
Department of Mechanical Engineering, Middle East Technical University, Ankara, Türkiye; Center for Gear, Power Transmission Systems and Vibration Research, Middle East Technical University, Ankara, Türkiye
e-mail: ender@metu.edu.tr; izzet.ulug@metu.edu.tr

Ludovic Renson et al. (eds.), *Nonlinear Structures & Systems, Vol. 1*, Conference Proceedings of the Society for Experimental Mechanics Series, https://doi.org/10.13052/97887-438-0146-7_15

expensive, especially for systems with nonlinearities like free-play. As shown by Conner et al. [3] and Trickey et al. [5], solving nonlinear equations in the time domain often requires significant computational resources due to the complexity of the simulations. In contrast, frequency-domain methods, such as the DFM, are more efficient for analyzing systems with periodic responses, providing accurate predictions of flutter behavior. This method linearizes the nonlinear system around limit cycles, allowing for the calculation of stability boundaries and LCOs without extensive simulations. Studies by Dowell and Tang [1] and Yurkovich [6] have demonstrated the advantages of frequency-domain approaches in handling nonlinear aeroelastic problems, offering accurate predictions of flutter dynamics. In a recent study, Frey et al. [7] compared time-domain and frequency-domain methods on turbine blades with nonlinear unsteady flow conditions in case, and demonstrated that frequency-domain solvers not only reduce the computational cost but also effectively model aeroelastic instabilities, especially under transonic flow conditions where strong shock interactions impact system dynamics.

The flutter characteristics of an airfoil with free-play nonlinearity at the control surface are explored using a three-degree-of-freedom (3-DOF) model. Free-play nonlinearity is represented by a piecewise linear stiffness element and the behavior of the system is studied in the frequency domain. This approach effectively predicts the flutter boundary and the onset of LCOs, providing a clearer understanding of how free-play affects system stability and post-flutter dynamics.

Mathematical Modelling

The 3-DOF airfoil model used in this study is given in Fig. 1. The airfoil exhibits three degrees of freedom: vertical motion (plunge), rotational motion around a horizontal axis (pitch), and control surface motion (flap), denoted by h, α, and β, respectively. The moments of inertia about the elastic axis for the airfoil and control surface are represented by I_α and I_β, respectively. Nonlinearity is introduced through torsional free-play at the control surface hinge, as previously studied and tested by Conner et al. [2]. The numerical parameters used in this paper were also adopted from Conner et al.'s study. Simple models, like the one shown in Fig. 1, are commonly used in similar analyses for their practicality.

As shown in Fig. 1, the model represents a two-dimensional airfoil placed in a steady horizontal airflow. Key parameters include the freestream velocity U, the semi-chord length b, stiffnesses in pitch, plunge, and control surface hinge directions (k_α, k_h, k_β), as well as the mass of the wing m_w, and the total mass of the system m_T. Additionally, the damping coefficients for the pitch, plunge, and flap motions are denoted as c_α, c_h and c_β, respectively, which describe the energy dissipation in each mode of motion.

The structural behavior is governed by linear bending and torsional springs along the airfoil's elastic axis and control surface hinge line, which simulate the restoring forces from the structure. Additionally, the distances between key points in the system —such as from elastic axis to the mid-chord a the mid-chord to the hinge line c, the elastic axis to the center of mass of the airfoil x_α, and the hinge line to the center of mass of the control surface x_β—are also considered. Finally, the total unsteady aerodynamic forces in the vertical direction, as well as the aerodynamic moments about the elastic axis and flap hinge, are represented by L, M_α and M_β, respectively.

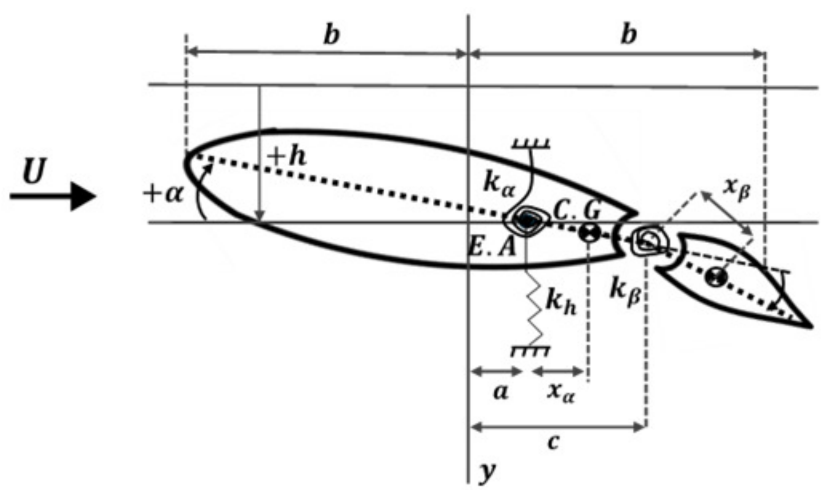

Fig. 1 Schematic of a 3-DOF aeroelastic wing section with pitch, plunge, and control surface spring restraints.

Equation of motion of the 3-DOF airfoil model given in Fig. 1 can be written as follows.

$$\mathbf{M}\left\{\begin{array}{c}\ddot{h}\\ \ddot{\alpha}\\ \ddot{\beta}\end{array}\right\}+\mathbf{C}\left\{\begin{array}{c}\dot{h}\\ \dot{\alpha}\\ \dot{\beta}\end{array}\right\}+\mathbf{K}\left\{\begin{array}{c}h\\ \alpha\\ \beta\end{array}\right\}=\left\{\begin{array}{c}L\left(h,\alpha,\beta\right)\\ M_{\alpha}\left(h,\alpha,\beta\right)\\ M_{\beta}\left(h,\alpha,\beta\right)\end{array}\right\}, \tag{1}$$

where, $\mathbf{M}$, $\mathbf{C}$ and $\mathbf{K}$ are the representatives of structural mass, stiffness, and damping of the system. The same system is considered in Fung [8] and equations of motion of the system given in Eq. (1) are the same. System matrices defined in Eq. (1) can be written explicitly as

$$\mathbf{M}=\begin{bmatrix} m_T & m_{wb}x_{\alpha} & m_{wb}x_{\beta}\\ m_{wb}x_{\alpha} & m_{wb}^2 r_{\alpha}^2 & m_{wb}^2 r_{\beta}^2+m_{wb}^2 x_{\beta}(c-a)\\ m_{wb}x_{\beta} & m_{wb}^2 r_{\beta}^2+m_{wb}^2 x_{\beta}(c-a) & m_{wb}^2 r_{\beta}^2\end{bmatrix} \tag{2a}$$

$$\mathbf{K}=\begin{bmatrix} k_h & 0 & 0\\ 0 & k_{\alpha} & 0\\ 0 & 0 & k_{\beta}(\beta)\end{bmatrix} \tag{2b}$$

$$\mathbf{C}=\begin{bmatrix} c_h & 0 & 0\\ 0 & c_{\alpha} & 0\\ 0 & 0 & c_{\beta}\end{bmatrix} \tag{2c}$$

This model builds on the state-space framework proposed by Edwards et al. [9]. Due to the free-play nonlinearity, which causes a piecewise linear variation in the structural stiffness of the control surface hinge, as illustrated in Fig. 2, the entire system can be described as a nonlinear combination of three linear subsystems. Understanding this nonlinearity is crucial in flutter analysis, as the presence of free-play significantly alters the dynamics of the system. Bai et al. [10] demonstrated that free-play affects flutter speed by causing sudden stiffness changes once the gap is closed, which reduces stability and lowers the flutter onset.

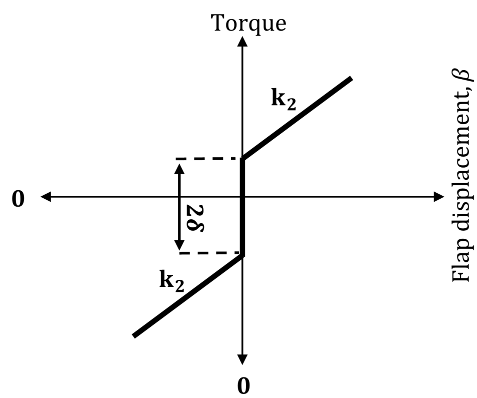

Fig. 2 Torque vs. flap displacement (β) in the presence of free-play nonlinearity.

The aerodynamic lift and moments L, M_{α} and M_{β} are calculated using the Theodorsen method, which employs linearized thin airfoil theory to evaluate unsteady aerodynamic forces and moments, as outlined in Theodorsen [11].

$$L\left(h,\alpha,\beta\right)=-\pi\rho b^2\left[\ddot{h}+U\dot{\alpha}-ba\ddot{\alpha}-\frac{U}{\pi}T_4\dot{\beta}-\frac{b}{\pi}T_1\ddot{\beta}\right]-2\pi\rho UbQC\left(k\right), \tag{3}$$

$$\begin{aligned}M_{\alpha}(h,\alpha,\beta)=\pi\rho b^2\Bigg[&ba\ddot{h}-Ub\left(\frac{1}{2}-a\right)\dot{\alpha}-b^2\left(\frac{1}{8}+a^2\right)\ddot{\alpha}-\frac{U^2}{\pi}(T_4+T_{10})\beta\\ &+\frac{Ub}{\pi}\left\{-T_1+T_8+(c-a)T_4-\frac{1}{2}T_{11}\right\}\dot{\beta}+b^2\pi\left\{T_7+(c-a)T_1\right\}\ddot{\beta}\Bigg]\quad+2\pi\rho b^2\left(a+\frac{1}{2}\right)QC(k),\end{aligned} \tag{4}$$

$$M_\beta\left(h,\alpha,\beta\right)=\pi\rho b^2\left[\frac{b}{\pi}T_1\ddot{h}+\frac{Ub}{\pi}\left\{2T_9+T_1-\left(a-\frac{1}{2}\right)T_4\right\}\dot{\alpha}-\frac{2b^2}{\pi}T_{13}\ddot{\alpha}-\left(\frac{U}{\pi}\right)^2\left(T_5-T_4T_{10}\right)W\beta\right]$$
$$+\frac{Ub}{2\pi^2}T_4T_{11}\dot{\beta}\;+\left(\frac{b}{\pi}\right)^2T_3\ddot{\beta}-\rho Ub^2T_{12}QC\left(k\right). \tag{5}$$

where Theodorsen's constants T_j are defined in [11], while $C\left(k\right)$ and Q are described as follows

$$C\left(k\right)=\frac{H_1^{(2)}\left(k\right)}{H_1^{(2)}\left(k\right)+iH_0^{(2)}\left(k\right)},\ \text{and}\ H_n^{(2)}=J_n\left(k\right)-iY_n\left(k\right) \tag{6}$$
$$Q=U\alpha+\dot{h}+\dot{\alpha}b\left(\frac{1}{2}-a\right)+\frac{U}{\pi}T_{10}\beta+\frac{b}{2\pi}T_{11}\dot{\beta}. \tag{7}$$

When flutter occurs, i.e. on the onset of flutter, the net damping in the system becomes zero and one of the vibration modes of the system follows a simple harmonic behavior. Due to the small amplitude of these oscillations, linear aerodynamic theory is adequate for modelling the unsteady air loads on a lifting surface in motion. Therefore, h, α and β can be represented as follows

$$\left\{\begin{array}{c}h\\ \alpha\\ \beta\end{array}\right\}=\left\{\begin{array}{c}\hat{h}\\ \widehat{\alpha}\\ \widehat{\beta}\end{array}\right\}e^{i\omega t}\,, \tag{8}$$

where ω is frequency of the motion and, $\hat{h}$, $\widehat{\alpha}$ and $\widehat{\beta}$ are complex amplitudes. Moreover, aerodynamic force and moments are functions of the generalized coordinates. By identifying h, α and β within the expressions for L, M_α and M_β, these terms can be arranged into matrices where the stiffness, damping, and mass matrices of the system can rewritten as follows

$$\mathbf{M}_\mathrm{a}=\begin{bmatrix}-\pi\rho b^2 & \pi\rho b^3a & \rho b^3T_1\\ \pi\rho b^3a & -\pi\rho b^4\left(\frac{1}{8}+a^2\right) & \rho b^4\left(T_7+(c-a)T_1\right)\\ \rho b^3T_1 & -2\rho b^4T_{13} & \frac{\rho b^4T_3}{\pi}\end{bmatrix} \tag{9a}$$

$$\mathbf{K}_\mathrm{a}=\begin{bmatrix}0 & -2\pi\rho U^2bC(k) & -2\rho U^2bT_{10}C(k)\\ 0 & 2\pi\rho b^2UC(k)\left(a+\frac{1}{2}\right) & 2\rho b^2UT_{10}C(k)\left(a+\frac{1}{2}\right)-\rho b^2U^2(T_4+T_{10})\\ 0 & -\rho U^2b^2T_{12}C(k) & -\dfrac{\rho b^2U^2\left(T_5-T_4T_{10}\right)+\rho U^2b^2T_{12}T_{10}C(k)}{\pi}\end{bmatrix} \tag{9b}$$

$$\mathbf{C}_\mathrm{a}=\begin{bmatrix}-2\pi\rho UbC(k) & -\pi\rho b^2U-2\pi\rho Ub^2C(k)\left(\frac{1}{2}-a\right) & \rho b^2UT_4-\rho Ub^2T_{11}C(k)\\ 2\pi\rho b^2\left(a+\frac{1}{2}\right)C(k) & 2\pi\rho b^3C(k)N_2-\pi\rho b^3U\left(\frac{1}{2}-a\right) & \rho b^3UN_1+\rho b^3\left(a+\frac{1}{2}\right)C(k)T_{11}\\ -\rho Ub^2T_{12}C(k) & \rho b^3UN_3-\rho Ub^3T_{12}C(k)\left(\frac{1}{2}-a\right) & \dfrac{\rho b^3U\left(T_{12}T_{11}C(k)-T_4T_{11}\right)}{2\pi}\end{bmatrix} \tag{9c}$$

where,

$$N_1=\left(-T_1+T_8+(c-a)T_4-\frac{1}{2}T_{11}\right),\quad N_2=\left(a+\frac{1}{2}\right)\left(a-\frac{1}{2}\right),\quad N_3=\left(3T_1-\left(a-\frac{1}{2}\right)T_4\right) \tag{9d}$$

Then, equation of motion can be written as follows:

$$\overline{\mathbf{M}}\ddot{\mathbf{x}}+\overline{\mathbf{C}}\dot{\mathbf{x}}+\overline{\mathbf{K}}\,\mathbf{x}=0, \tag{10}$$

where,

$$\overline{\mathbf{M}}=\mathbf{M}-\mathbf{M}_a,\quad \overline{\mathbf{C}}=\mathbf{C}-\mathbf{C}_a,\quad \overline{\mathbf{K}}=\mathbf{K}-\mathbf{K}_a \tag{11a}$$
$$\mathbf{x}=\{h\ \alpha\ \beta\} \tag{11b}$$

Nonlinear Flutter Solution

The nonlinear flutter solution is obtained by using the state-space approach and solved through incrementally increasing free-stream velocity, as shown by Kösterit et al. [12]. Eigenvalue analysis is conducted within the state-space formulation, where the real parts of the eigenvalues are examined to identify the flutter speed. Depending on the value of eigenvalue λ, behavior of the system may exhibit oscillatory, dissipative, or dispersive behavior. If $\lambda < 0$, the system is dynamically stable; if $\lambda > 0$, it becomes dynamically unstable, leading to divergent oscillations. The point where $\lambda = 0$ defines the 'stability boundary.' In aeroelastic systems, this instability is known as 'flutter', and the corresponding boundary is called the 'flutter boundary'. In flutter cases, the solution typically shows oscillatory or dispersive behavior, both indicating instability, where even a small disturbance can lead to large structural displacements. Hence, the flutter speed is determined as the point where the real part of the eigenvalue transitions from negative to positive. In state space form, equation of motion of the system can be written as follows:

$$\mathbf{A}\dot{\mathbf{q}} + \mathbf{B}\mathbf{q} = 0 \tag{12a}$$

$$\mathbf{A} = \begin{bmatrix} 0 & \overline{\mathbf{M}} \\ \overline{\mathbf{M}} & \overline{\mathbf{C}} \end{bmatrix}, \quad \mathbf{B} = \begin{bmatrix} -\overline{\mathbf{M}} & 0 \\ 0 & \overline{\mathbf{K}} \end{bmatrix}, \quad \mathbf{q} = \begin{Bmatrix} \dot{\mathbf{x}} \\ \mathbf{x} \end{Bmatrix} \tag{12b}$$

Here, q assuming harmonic form for x, q can be represented as follows

$$\mathbf{q} = \mathbf{q}e^{\lambda t}, \tag{13a}$$

Substituting Eq. (13a) into Eq. (12a) the following eigenvalue problem is obtained

$$\lambda\mathbf{A}\mathbf{q} + \mathbf{B}\mathbf{q} = 0. \tag{13b}$$

Eq. (13b) is for the linear problem. For the nonlinear problem, DFM is used to find the nonlinear stiffness matrix. This method, as demonstrated by Iannelli et al. [13], allows for stability assessment without requiring detailed frequency-domain analysis. In their study, Iannelli et al. applied DFM to aeroelastic systems with free-play nonlinearities, addressing uncertainties using structured singular values and integral quadratic constraints. Their work effectively captured the dynamic behavior of aeroelastic systems, providing an efficient way to model and analyze nonlinearities such as free-play in control surfaces. In the presence of free-play nonlinearity, the nonlinear restoring torque acting on the control surface can be written as follows by using the describing function theory

$$T_N = \nu \bullet \widehat{\beta}, \tag{14}$$

where, ν is the describing function which is defined as

$$\nu = \frac{i}{\pi A}\int_0^{2\pi} T_N\left(Asin\left(\psi\right)\right)e^{-i\psi}d\psi. \tag{15}$$

T_N is the nonlinear restoring torque, A is the amplitude of oscillations, $\psi = \omega t$ and $\widehat{\beta}$ is the complex representation of the flap displacement. It should be noted that, in general, ν is complex quantity; however, for free play nonlinearity, it is a real quantity, and it can be obtained as follows

$$\nu\left(A\right) = \begin{cases} \frac{-2k_2}{\pi}\left(\sin^{-1}\left(\frac{\delta}{A}\right) + \frac{\delta}{A}\sqrt{1-\left(\frac{\delta}{A}\right)^2}\right) + k_2 & A > \delta \\ 0 & A \leq \delta \end{cases}, \tag{16}$$

Here, A is the flap displacement amplitude, k_2 is the torsional stiffness of the hinge mechanism, and δ defines the gap in free-play at one side of the equilibrium resulting total gap of 2δ. Using DFM, the stiffness matrix of the system can be written as follows

$$\overline{\mathbf{K}} = \mathbf{K} - \mathbf{K_a} + \begin{bmatrix} 0 & 0 & 0 \\ 0 & 0 & 0 \\ 0 & 0 & \nu\left(\beta\right) \end{bmatrix}. \tag{17}$$

Results

The flutter characteristics of the system are influenced by several structural and geometric parameters, which affect both flutter speed and frequency. The interaction between these parameters and the aeroelastic response is critical for understanding the stability of the system. The results demonstrate how variations in stiffness, semi-chord length, and hinge line position shape susceptibility to flutter, providing insights into optimizing aeroelastic performance.

Table 1 System parameters used in flutter analysis

Geometric Parameters	
b	$0.127\ [m]$
a	$-0.5\ [m]$
c	$0.5\ [m]$
Mass Parameters	
m_w	$0.62868\ [kg]$
m_T	$1,76435\ [kg]$
Inertial Parameters	
x_a	$0.434\ [m]$
x_b	$0.01996\ [m]]$
I_α	$0.0137\ [kg\ m^2]$
I_β	$0.0003264\ [kg\ m^2]$

First, linear flutter solution is obtained and given in Fig. 3. The real and imaginary parts of the eigenvalue provide the flutter speed and frequency, respectively. From the analysis, it is observed that the plunge mode reaches flutter at a speed of 22.72 m/s where the real part of the eigenvalue reaches zero with a corresponding frequency of 5.74 Hz. The system parameters used in the solution are provided in Table 1.

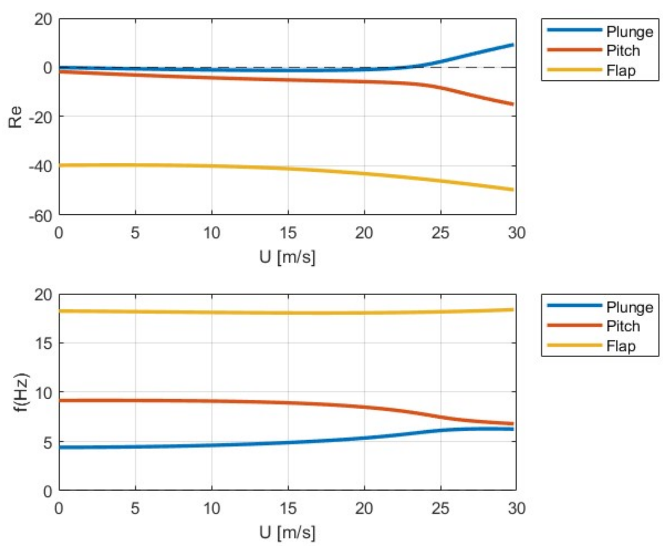

Fig. 3 Variation of real and imaginary parts of the eigenvalues vs. freestream velocity for pitch, plunge, and flap modes.

The nonlinear problem is considered next. As stiffness increases ($k = 10,\ 25,\ 100\ [N/m]$), the flutter speed increases significantly after exceeding the free-play limit. This effect is illustrated in Fig. 4a, which shows the sharp increase in flutter speed, indicating a more stable system with higher stiffness. However, up to around 2 degrees of rotational displacement, the flutter speed remains unchanged. This behavior is a direct result of the free-play that was introduced in the model. The gap allows for initial motion without engaging the stiffness; and as a result, the system does not exhibit any change in flutter speed within this range. Once the rotational displacement exceeds the free-play limit, the stiffness engages, leading to a sharp increase in flutter speed. After this point, the curves become steeper, showing a more abrupt transition to flutter with higher stiffness values. This outcome aligns with the idea that increased stiffness enhances the stability of the system, making it less prone to aeroelastic instabilities. The next analysis focuses on the semi-chord length b as shown in Fig. 4b. As the semi-chord length increases, both the flutter speed and frequency show a slight increase. This can be attributed to changes in the distribution of aerodynamic forces along the airfoil. Although the effect of semi-chord length is more subtle compared to stiffness, it still plays a role in stabilizing the system. Larger semi-chord lengths result in a marginally higher resistance to flutter, particularly when aerodynamic loads are distributed across the control surface.

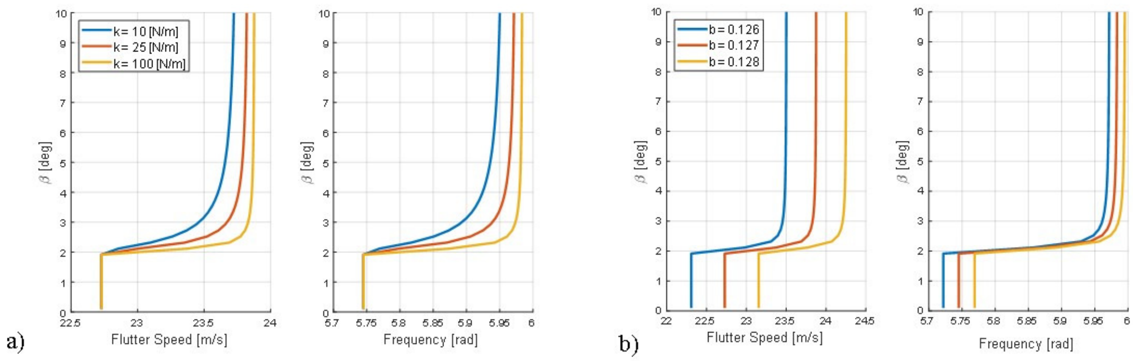

Fig. 4 Variation of flutter speed and frequency with respect to a) stiffness and b) chord length.

When evaluating the hinge line distance, c, a more significant influence on flutter behavior is observed, which is illustrated in Fig. 5. As c increases, both flutter speed and frequency decrease noticeably. This indicates that the system becomes more susceptible to flutter at lower speeds as the hinge line moves further from the mid-chord. This shift alters the torsional dynamics of the airfoil, making the structure more sensitive to aeroelastic forces. The positioning of the hinge line is therefore a critical design consideration for managing flutter risk in practical applications. Lastly, the distance between the elastic axis and the mid-chord, a, shows a similar trend. As a increases, both flutter speed and frequency decrease slightly. This suggests that as the elastic axis moves further from the mid-chord, the system becomes more prone to flutter. While the effect of a is less pronounced than that of stiffness or hinge line position, it still plays an important role in the overall stability of the system. Adjusting this parameter in combination with others can help optimize the aeroelastic performance of the system.

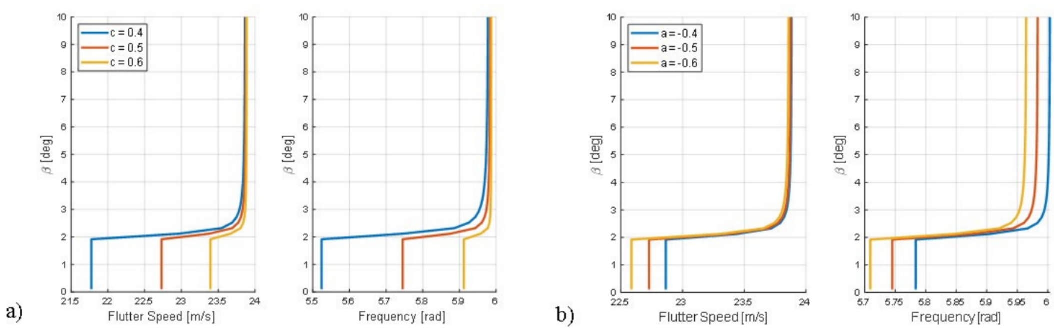

Fig. 5 Variation of flutter speed and frequency with respect to a) hinge line distance and b) elastic axis location.

Conclusion

This study focuses on analyzing the flutter behavior of a 3-DOF airfoil model with control surface free-play. Describing Function Method (DFM) is used to capture the nonlinear dynamics. The results indicate that free-play significantly affects both the flutter speed and the aeroelastic response of the system. Initially, control surface moves within the free-play gap without activating the stiffness, resulting in no change in flutter speed over a specific range of rotational displacement. Once the stiffness engages, there is a sharp increase in flutter speed, indicating a faster transition to instability in stiffer systems. It is observed from free-play affects aeroelastic behavior significantly, highlighting the importance of optimizing structural system parameters to reduce the vulnerability to flutter.

References

1. E. H, Dowell and D. M. Tang, “Aeroelastic response induced by free play, Part 2: Theoretical/experimental correlation analysis,” *AIAA Journal*, vol. 49, no. 11, pp. 2543–2554, 2011.

2. Q. Yu, Y. Zhang, and Y. Wang, “Numerical analysis of free-play-induced aeroelastic phenomena: A numerical approach with adaptive step size control,” *Int. J. Aerosp. Eng.*, vol. 2024, pp. 1–13, Apr. 2024.
3. M. D. Conner, D. M. Tang, E. H. Dowell, and L. N. Virgin, “Nonlinear behavior of a typical airfoil section with control surface freeplay: A numerical and experimental study,” *Journal of Fluids and Structures*, vol. 11, no. 1, pp. 89–109, 1997.
4. S. Irani and S. Sazesh, “A new flutter speed analysis method using stochastic approach,” *Journal of Fluids and Structures*, vol. 40, pp. 105–114, 2013.
5. S. T. Trickey, L. N. Virgin, and E. H. Dowell, “Characterizing stability of responses in a nonlinear aeroelastic system,” in 41st Structures, Structural Dynamics, and Materials Conference and Exhibit, Dec. 2000.
6. R. Yurkovich, “Nonlinear Aeroelasticity and Flutter Suppression Using Frequency Domain Techniques,” presented at the 20th International Forum on Aeroelasticity and Structural Dynamics (IFASD), June 2004.
7. C. Frey, G. Ashcroft, H. Kersken, and D. Schlüß, “Flutter analysis of a transonic steam turbine blade with frequency and time-domain solvers,” *Int. J. Turbomach. Propuls. Power*, vol. 4, no. 2, pp. 15, Jun. 2019.
8. Y. C. Fung, An Introduction to the Theory of Aeroelasticity, Dover Publications, 1993.
9. J. W. Edwards, M. P. Conner, and T. W. Strganac, “Aeroelastic dynamic response and control of an airfoil section,” Journal of Aircraft, vol. 16, no. 3, pp. 65–74, 1979.
10. L. Bai, Z. Wu, and C. Yang, “Nonlinear Aeroelastic Characteristics of a Supersonic All-Movable Fin with Single or Multiple Freeplay Nonlinearities,” Aerospace, vol. 10, no. 1, pp. 1–20, 2023.
11. T. Theodorsen, “General theory of aerodynamic instability and the mechanism of flutter,” *NACA Report 496*, 1935.
12. G. Kösterit and E. Ciğeroğlu, “Determination of flutter speed of 2D nonlinear wing by using describing function method and state-space formulation,” *presented at the 40th Conference and Exposition on Structural Dynamics (IMAC)*, Florida, United States, 2023.
13. A. Iannelli, A. Marcos, and M. Lowenberg, “Nonlinear flutter analysis with uncertainties based on Describing Function and Structured Singular Value with an IQC validation,” in *Proc. 7th European Conf. Aeronautics and Aerospace Sciences (EUCASS)*, pp. 1–12, Milan, Italy, 2017.